A Unified Theoretical Model for Breakup of Bubbles and Droplets in Turbulent Flows

Chutian Xing, Tiefeng Wang, Kunyu Guo, and Jinfu Wang
Beijing Key Laboratory of Green Reaction Engineering and Technology, Dept. of Chemical Engineering, Tsinghua University, Beijing 100084, China

DOI 10.1002/aic.14709
Published online December 21, 2014 in Wiley Online Library (wileyonlinelibrary.com)

Pressure has a significant effect on bubble breakup, and bubbles and droplets have very different breakup behaviors. This work aimed to propose a unified breakup model for both bubbles and droplets including the effect of pressure. A mechanism analysis was made on the internal flow through the bubble/droplet neck in the breakup process, and a mathematical model was obtained based on the Young–Laplace and Bernoulli equations. The internal flow behavior strongly depended on the pressure or gas density, and based on this mechanism, a unified breakup model was proposed for both bubbles and droplets. For the first time, this unified breakup model gave good predictions of both the effect of pressure or gas density on the bubble breakup rate and the different daughter size distributions of bubbles and droplets. The effect of the mother bubble/droplet diameter, turbulent energy dissipation rate and surface tension on the breakup rate, and daughter bubble/droplet size distribution was discussed. This bubble breakup model can be further used in a population balance model (PBM) to study the effect of pressure on the bubble size distribution and in a computational fluid dynamics-population balance model (CFD-PBM) coupled model to study the hydrodynamic behaviors of a bubble column at elevated pressures. © 2014 American Institute of Chemical Engineers *AIChE J*, 61: 1391–1403, 2015
Keywords: bubble/droplet breakup, pressure, daughter size distribution, internal flow through bubble/droplet neck, turbulent flows

Introduction

Bubble column reactors are operated under high pressure in a variety of chemical processes, such as hydrocracking of petroleum residue (5–21 MPa), Fischer-Tropsch synthesis (1–5 MPa), benzene hydrogenation (5 MPa), and oxidation of para-xylene to terephthalic acid (0.3–3 MPa).[1–8] In the last three decades, many researchers have found that pressure has a significant effect on the hydrodynamics of bubble columns. At elevated pressures, the gas holdup significantly increases due to a decrease in the stable bubble size, which in turn increases the number of small bubbles.[1,3,9–14] Wilkinson and Vondierendonck[1] found that the effects of both pressure and molecular weight of gas on the gas holdup were caused by the same factor of gas density and the bubble breakup rate increased with increasing gas density. This conclusion was confirmed by subsequent researchers.[7,15–18] In addition, the experimental data of Wilkinson and Vondierendonck[1] showed that the effect of gas density on the gas holdup was nonlinear. When the gas density was below a particular value, the change of gas density had a small influence on the gas holdup, and beyond that value, the gas holdup increased with increasing gas density. Some researchers investigated the effect of pressure on the gas phase structure using the dynamic gas disengagement method.[19,20] They found that with increasing pressure the holdup of large bubbles was almost unchanged but the holdup of small bubbles significantly increased. The radial profile of the gas holdup became flatter[14] and the axial liquid dispersion coefficient decreased with increasing pressure.[4] The rising velocity of single bubbles in liquids and liquid-solid suspensions decreased with increasing pressure[21] and the slip velocity of bubble swarms also decreased with increasing pressure and finally approached that of small bubbles.[17,20] The bubble trajectory was more tortuous at high pressure than at low pressure in a three-phase fluidized bed.[22] In addition, the transition point from the homogeneous to heterogeneous regime shifted to higher gas velocities at elevated pressures.[9,14] Dewes and Schumpe[18] found that the volumetric mass-transfer coefficient significantly increased with increasing pressure.

Besides the intensive studies in bubble columns, the effect of pressure or gas density also received much attention from other aspects, such as the bubble pinch-off behavior and laser-induced bubble dynamics. Keim[23] studied the pinch-off behavior of a bubble from an underwater nozzle and found that the gas density affected the axial asymmetry of the neck near pinch-off. For denser gases, the internal flow through the bubble neck late in the collapse process significantly changed the pinch-off dynamics. Li et al.[24] investigated the effect of pressure on the dynamics of laser-induced bubbles and found that both the maximum bubble size and bubble collapse time decreased nonlinearly with increasing pressure.

Correspondence concerning this article should be addressed to T. Wang at wangtf@tsinghua.edu.cn.

Although many experimental works have been reported on the effect of pressure in bubble columns, very limited works have been reported on the mechanism of pressure effect. Previous research shows that bubble coalescence is not affected by pressure,[1,25,26] therefore more attentions are paid to the effect of pressure on bubble breakup. Krishna et al.[6] proposed that increasing gas density reduced the interaction between neighboring bubbles and decreased the chance of instability propagation. Wilkinson and Vondierendonck,[1] Letzel,[17] and Lin et al.[27] applied the Kelvin–Helmholz stability theory to model the effect of pressure on bubble breakup by considering the relative motion between the gas and liquid phases. Letzel[17] proposed that increasing gas density increased the growth factor of the unstable surface waves. The surface of large bubbles became unstable for a wider range of wave, and as a result, large bubbles broke into smaller bubbles. The rise velocity of large bubbles was predicted to be inversely proportional to the square root of the gas density if bubbles with different gas densities have the same spectrum of growth factors.[10,17] Fan and his coworkers argued that Rayleigh–Taylor and Kelvin–Helmholtz instabilities alone were not the reason for the decreased bubble size with increasing pressure.[3,21,27] They proposed that the bubble breakup was caused by the centrifugal force when it exceeded the surface-tension force, especially at higher gas densities. Kemoun et al.[14] proposed that the decreased bubble size at elevated pressures was caused by both decreased bubble coalescence and enhanced bubble breakup. However, the important phenomenon that gas can flow through the bubble neck with a relatively high velocity has not yet been considered in the literature to model the effect of pressure on the hydrodynamics of bubble columns.[28,29] The effect of the internal flow through the neck on the bubble pinch-off behavior has been studied.[23,30–33] Ravelet et al.[34] studied the bubble breakup with a high speed camera in a turbulent flow. In that work, the experiments were well controlled to give high-quality results. The visualization volume was surrounded by a square glass box filled with water to minimize optical distortions. The images were taken at a rate of 300 Hz, and the number of pixels inside a typical bubble was around 3000. From their images of bubble breakup, the gas flow velocity through the neck of a bubble of 10 mm (U_{neck}) was estimated to be 2.4 m/s, which was much larger than the bubble rise velocity. Recently, Zhao and Ge[35] investigated the influence of pressure on the bubble breakup and bubble size distribution with the population balance model (PBM). They introduced a concept of eddy efficiency and indicated that the bubble breakup rate increased with increasing gas density due to the increase of bubble oscillation period. However, the effect of gas density on the predicted bubble breakup rate was much less pronounced than the experimental results.

Although the influence of pressure on the hydrodynamics of bubble columns is pronounced and this is very important for the design and scale-up of reactors at high pressures, the underlying mechanism has not been well understood and most studies have been limited to qualitative or semiquantitative analysis. In addition, the breakup behaviors are very different for bubbles and droplets. The experimental results of Hesketh et al.[36] and Andersson and Andersson[29] show that unequal fragments for bubble breakup are often formed, and hence, the daughter bubble size distribution is typically M-shaped. In contrast, when only binary breakup is considered for droplets, the most probable outcome is equal-sized breakup and hence the daughter droplet size distribution is typically Λ-shaped, which is supported by the experimental results of Andersson and Andersson[29] and Zaccone et al.[37] This work aimed to explain and study the effect of pressure or gas density on both the bubble/droplet breakup rate and daughter size distribution. A new unified breakup model was proposed for both bubbles and droplets by including the mechanism of internal flow through the neck of bubble/droplet. Good predictions were obtained on the nonlinear effect of the gas density on the bubble breakup rate and the different daughter size distributions of bubbles and droplets. Our previous works have shown that the bubble breakup and coalescence models are critical to properly predict the bubble size distributions by the PBM[38] and consequently important to predict the hydrodynamic behaviors of a bubble column with a CFD-PBM coupled model.[39,40] Therefore, the new bubble breakup model that includes the effect of pressure will be very useful for the simulation of industrial bubble columns operated at high pressures.

Model Development

In a fully developed turbulent flow, the breakup of a bubble/droplet is mainly caused by turbulent eddy collision.[41] A bubble/droplet will deform when it is hit by a turbulent eddy, as shown in Figure 1. Because the breakup process is very complex, the following simplifications and assumptions were used in this work to develop the breakup model.

1. Only binary breakup is considered, which has been widely used in the literature.[35,36,41–43] This is because that the probability of binary bubble breakup is high (typically larger than 95%) according to the experimental results of Hesketh et al.[36] and Andersson and Andersson.[29] In contrast, for droplet breakup when the viscous effects are not negligible,[29] multiple breakup is frequent and the most frequent outcome of breakage is two equal-sized droplets and a satellite droplet. Considering that the volume of the satellite droplets is negligible, binary breakup is still a reasonable assumption.[29] Therefore, only binary breakup is considered in this work for bubble/droplet breakup.

2. Bubble/droplet breakup is mainly caused by collision with turbulent eddies.[41–43]

3. The deformed bubble/droplet can be divided into three parts: the smaller spherical part with a radius of R_1, the larger part with a radius of R_2, and the cylindrical neck part with diameter of d_{neck}.

4. Compared to the entrance and exit losses of bubble neck, the frictional loss along the bubble neck is ignored. Although R_1 and R_2 change in time during the internal flow, an average velocity U_{neck} is used to estimate the internal flow time scale t_1. Detailed discussion on this assumption is given in the third section.

5. The accelerating time for the fluid in rest from the beginning due to the pressure difference can be neglected compared with the time scale of internal flow.

6. When $R_1 = R_2$, the internal flow cannot be initiated and results in a singularity point. To avoid this mathematical irrationality, a small difference is set between R_1 and R_2, that is, $R_1 = (1-\delta)R_2$. $\delta = 0.02$ is used for the case of $R_1 = R_2$ in all calculations.

7. The minimum breakup fraction $f_{\text{v,min}}$ is determined by considering the internal flow, and the maximum breakup fraction $f_{\text{v,max}}$ is set to be 0.5. A model assumption that the modified breakup fraction decays by $\exp(-5f_{\text{v}})$ is used.

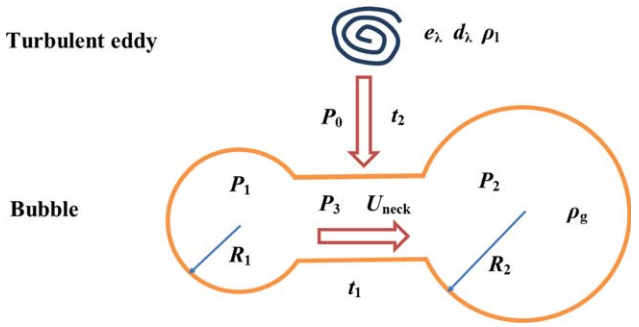

Figure 1. Sketch of the dynamic process of a bubble/droplet breakup.

[Color figure can be viewed in the online issue, which is available at wileyonlinelibrary.com.]

In this work, the bubble/droplet breakup was modeled in three steps. The breakup model without the internal flow through the bubble/droplet neck was first considered. Then in the second step, a physical model was proposed for the internal flow through the bubble/droplet neck, which in turn was quantitatively described by mathematical equations. In the final step, the effect of the internal flow was included in the breakup model to calculate the breakup rate and daughter size distribution at different pressures.

Breakup rate without internal flow through the bubble/droplet neck

Following Luo and Svendsen[42] and Wang et al.,[41] the specific rate that a bubble/droplet of size d breaks up with a breakup fraction of $f_v^{'}$ is expressed as

$$\Omega(f_v^{'}|d)=\int_{\lambda_{\min}}^{\lambda_{\max}} P_b(f_v^{'}|d,\lambda)\varpi_\lambda(d)\mathrm{d}\lambda \tag{1}$$

where $\varpi_\lambda(d)$ is the collision frequency, and the probability density $P_b(f_v^{'}|d,\lambda)$ is that a bubble/droplet with size d breaks into two bubbles, one has a volume of $vf_v^{'}$ and the other has a volume of $v(1-f_v^{'})$, when the bubble collides with a turbulent eddy of size λ.

In Eq. 1, the lower limit of integral is often taken to be 11.4–31.4 times the Kolmogorov scale.[35,41–44] Regarding the upper limit of integral, many researchers[35,41,42] used the diameter of the bubble/droplet with the consideration that eddies larger than this size merely transport the bubble/droplet. However, recent research showed that the upper scale $\lambda_{\max}$ could be larger than the size of bubble/droplet d_b, because the eddy energy could be partially transferred.[43,44] Han et al.[43] reported that eddies of $\lambda \le 3d_b$ contributed to most of the bubble breakups while eddies of $\lambda \ge 5d_b$ had little contribution. Therefore, $\lambda_{\max}$ was taken to be $3d_b$ in this work.

Breakup Probability. The probability for a bubble/droplet of size d to break into a size of $d_1=f_{v1}^{1/3}d$ when the bubble/droplet interacts with an arriving eddy of size λ, is equal to the probability of the arriving eddy of size λ having a kinetic energy greater than or equal to the critical energy required for the bubble/droplet breakup. Experimental results show that the droplets turbulent velocity in a turbulent flow follows a normal distribution.[45] By introducing the assumption that turbulent eddies behave like droplets of the same size in a turbulent flow, Luo and Svendsen[42] proposed that turbulent eddies also have a normal velocity distribution. The normal velocity distribution of turbulent eddies has been widely used by Lee et al.,[46] Prince and Blanch,[47] Hagesaether et al.,[48] Wang et al.,[41] and Han et al.,[43] as reviewed by Solsvik et al.[49] The normal velocity distribution can also be obtained by analogy of turbulent eddies with gas molecules. Didier et al. pointed out that just as gas molecules almost always have a nearly normal velocity distribution, it appears that turbulence tends toward a similar universality in its stochastic structure.[50] Although this analogy is not strictly correct, it is a good approximation in many flow situations. Therefore, the assumption of normal velocity distribution is also used in this work. This is equivalent to the exponential-energy density function $P_e(e(\lambda))=\frac{1}{\bar{e}(\lambda)}\exp\left(-e(\lambda)/\bar{e}(\lambda)\right)$[47] and gives the following the probability density for a bubble/droplet of size d breaking with breakup fraction $f_v^{'}$ when hit by a turbulent eddy of size λ[42,43]

$$P_b(f_v^{'}|d,\lambda)=1-\int_0^{\chi_c}\exp(-\chi)d\chi=\exp(-\chi_c) \tag{2}$$

where χ is the dimensionless eddy energy, and the χ_c is the critical dimensionless energy for breakup. Wang et al. proposed that bubble breakup must satisfy both the surface energy constraint and capillary force constraint.[41,43] The following equation proposed by Han et al.[43] was used to calculate χ_c

$$\chi_c=\frac{e_{\text{critical}}(\lambda)}{\bar{e}(\lambda)}=\frac{\max(c_f,c_d)\pi d_b^2\sigma}{1/2\rho_l\bar{u}_\lambda^2\lambda^3}\begin{cases}1, & \lambda\le d_b\\ 1/4(\lambda/d_b)^2\sin^4(\pi d_b/(4\lambda)), & \lambda>d_b\end{cases} \tag{3}$$

where $c_f=(f_v^{'})^{2/3}+(1-f_v^{'})^{2/3}$ and $c_d=(\min(f_v^{'},1-f_v^{'}))^{-1/3}-1$ are the energy constraint[41,43] and capillary force constraint[43] for bubble/droplet breakup, respectively.

Collision Frequency. Based on Luo and Svendsen[42] and our previous study,[41] the collision frequency of the eddies with size $\lambda \le d_b$ can be determined by analogy with gas kinetic theory

$$\varpi_\lambda(d)=\frac{\pi}{4}(d+\lambda)^2\bar{u}_\lambda n_\lambda n \tag{4}$$

where n_λ is the number density of eddies with size λ, and it is calculated by

$$n_\lambda=\frac{0.822(1-\alpha_d)}{\lambda^4} \tag{5}$$

Equation 5 is a result of the kinetic energy spectrum for the inertial subrange of turbulence, $E(\kappa)=C\varepsilon^{2/3}\kappa^{-5/3}$, which was given by Batchelor[51] and has been validated by experiments.[52] The factor $(1-\alpha_d)$ is introduced because the volume of continuous phase is reduced due to the existence of dispersed phase and the turbulence eddies only exist in the continuous phase. The detailed deduction of Eq. 5 has been reported by Luo and Svendsen.[42]

The mean turbulent velocity of eddies with size λ is

$$\bar{u}_\lambda=\sqrt{2}(\varepsilon\lambda)^{1/3} \tag{6}$$

Substitution of Eqs. 5 and 6 into Eq. 4 gives

$$\varpi_\lambda(d)=0.923(1-\alpha_g)n\varepsilon^{1/3}\frac{(\xi+1)^2}{\mathrm{d}^{5/3}\xi^{11/3}} \tag{7}$$

For eddies with size $\lambda > d_b$, Andersson and Andersson[44] proposed an interaction frequency that was proportional to the bubble/droplet volume and argued that the arriving eddy containing enough kinetic energy could break the bubble/droplet during the eddy turn over time or lifetime, τ_e. Then the interaction frequency is defined as

$$\varpi_\lambda(d)=\frac{\pi d_b^3/6}{\max(\tau_e,\lambda/\bar{u})}n_\lambda n \tag{8}$$

where $\bar{u}$ is the mean turbulent velocity at a distance of d_b, and is expressed as[43]

$$\bar{u}=2\xi\sin^2(\pi/(4\xi))\bar{u}_\lambda \tag{9}$$

where $\xi = \lambda/d_b$.

Substitution of Eq. 9 into Eq. 8 gives

$$\varpi_\lambda(d)=\frac{0.43(1-\alpha_g)n\varepsilon^{1/3}}{\xi^{14/3}d^{5/3}\max\left\{1,1/\left[2\sqrt{2}\xi\sin^2(\pi/(4\xi))\right]\right\}} \tag{10}$$

Internal flow through the neck of bubble/droplet

As shown in Figure 1, the pressure inside the spherical parts P_i can be described by the Young–Laplace equation

$$P_i=P_0+\frac{2\sigma}{R_i}(i=1,2) \tag{11}$$

where P_0 is the pressure outside the bubble/droplet, and σ is the surface tension. Then, the pressure difference between the two spherical parts is given by

$$P_1-P_2=2\sigma\left(\frac{1}{R_1}-\frac{1}{R_2}\right) \tag{12}$$

Due to pressure difference, the fluid (gas for bubble and liquid for droplet) flows from the smaller part to the larger part through the bubble/droplet neck with a velocity U_{neck}, which can be described by the Bernoulli equation[53]

$$P_1=P_3+\frac{1}{2}\rho U_{neck}^2+\zeta_1\frac{1}{2}\rho U_{neck}^2 \tag{13}$$

$$P_3+\frac{1}{2}\rho U_{neck}^2=P_2+\zeta_2\frac{1}{2}\rho U_{neck}^2 \tag{14}$$

Combination of Eqs. 12 to 14 gives

$$U_{neck}=\sqrt{\frac{4\sigma}{(\zeta_1+\zeta_2)\rho}\left(\frac{1}{R_1}-\frac{1}{R_2}\right)} \tag{15}$$

where ζ_1 and ζ_2 are the local loss coefficients of contraction and expansion, respectively. According to Perry and Green,[53] ζ_1 can be estimated by $\zeta_1 = 0.5(1–d_{neck}^2/(4R_1^2))$, giving $\zeta_1 = 0.375$ for $d_{neck}/R_1 = 1$. Considering that the transition between the smaller bubble part and the bubble neck is not sharp-edged, a smaller value $\zeta_1 = 0.2$ was used in this work, and the local loss coefficient of expansion was chosen as $\zeta_2 = 0.3$.

The frictional head loss along the bubble neck is ignored in Eqs. 13 and 14 because it is much smaller than those of contraction and expansion. From Darcy–Weisbach equation,[53] the frictional loss coefficient is

$$\zeta_0=\kappa\frac{l_{neck}}{d_{neck}}=\frac{64}{\mathrm{Re}}\frac{l_{neck}}{d_{neck}} \tag{16}$$

where κ is the friction factor, and Re is the Reynolds number defined as

$$\mathrm{Re}=\frac{d_{neck}U_{neck}\rho_g}{\mu_g}=\sqrt{\frac{4\sigma\rho_gR_1}{(\zeta_1+\zeta_2)\mu_g^2}\left(1-\frac{R_1}{R_2}\right)} \tag{17}$$

For $R_1/R_2 \approx 0$, $R_1 = 0.002$ m, $\mu_g = 1.79 \times 10^{-5}$ Pa s, $\rho = 1.27$ kg/m^3 and $\sigma = 0.072$ N/m, Re $\approx$ 1900. In the breakup process, l_{neck}/d_{neck} is usually smaller than 1, then $\zeta_0 << \zeta_1$ and ζ_2.

The time for the smaller part to completely flow into the larger part is estimated as

$$t_1=\frac{V_1}{U_{neck}\pi d_{neck}^2/4} \tag{18}$$

where V_1 is the volume of the smaller part of the bubble/droplet.

In Eq. 18, the accelerating time for the fluid in rest from the beginning is neglected, because the accelerating time is estimated to be much smaller than the time t_1 using the governing equation $\rho\frac{\partial U}{\partial t}+\frac{\partial P}{\partial z}=-\kappa\rho\frac{U|U|}{2d_{neck}}$ proposed by Tijsseling[54] for the unsteady flow in a horizontal cylinder. Using this governing equation, the ratio between the accelerating time for the fluid to the time of internal flow, t_{accel}/t_1, is shown to be independent of ΔP, because ΔP is the driving forces for both fluid acceleration and internal flow. For $\zeta_1 + \zeta_2 = 0.5$, $\kappa = 0.02$, and $l_{neck}/d_{neck} = 0.4$, t_{accel}/t_1 is estimated to be less than 0.30.

In addition to the internal flow through the bubble/droplet neck, the bubble neck shrinking is also affected by its interaction with the hitting turbulent eddies. According to Wilkinson et al.,[28] the pressure in the bubble neck decreases due to the internal gas flow, and this lower pressure acts as a suction force on the interface of the bubble neck, which in principle, enhances the contraction of the bubble neck. From Eqs. 11 to 15, the net dynamic pressure $P_0 - P_3$ acting on the interface of the bubble neck can be calculated by

$$P_0-P_3=\frac{1}{2}\rho U_{neck}^2+\frac{1}{2}\zeta_1\rho U_{neck}^2-\frac{2\sigma}{R_1}=\frac{2\sigma}{\zeta_1+\zeta_2}\left(\frac{1-\zeta_2}{R_1}-\frac{1+\zeta_1}{R_2}\right) \tag{19}$$

The value of $P_0 - P_3$ can be positive or negative, depending on the values of ζ_1, R_1, and R_2. When the value of $P_0 - P_3$ is positive, the dynamic pressure acts on the bubble neck and enhances the contraction of the bubble neck. Otherwise, the dynamic pressure acts on the hitting eddy and prevents the contraction of the bubble neck.

This net dynamic pressure exerts an additional shrinking velocity U_{plus} on the bubble neck surface, which can be calculated by

$$U_{plus}=\begin{cases}\sqrt{\dfrac{2(P_0-P_3)}{\rho_g}}, & P_0-P_3>0\\ -\sqrt{\dfrac{-2(P_0-P_3)}{\rho_l}}, & P_0-P_3\le 0\end{cases} \tag{20}$$

The bubble neck shrinking velocity is the sum of the turbulent eddy velocity U_λ and the additional velocity U_{plus}. Therefore, the time t_2 for shrinking of bubble neck is estimated as

$$t_2=\begin{cases}\dfrac{d_{\text{neck}}}{U_{\text{plus}}+U_\lambda}, & U_{\text{plus}}+U_\lambda>0\\ +\infty, & U_{\text{plus}}+U_\lambda\le 0\end{cases} \tag{21}$$

where U_λ is the velocity of a turbulent eddy. For a turbulent eddy with size λ and kinetic energy $e(\lambda)$, U_λ is calculated as

$$U_\lambda=\sqrt{\frac{12}{\pi}\frac{e(\lambda)}{\rho_c d_\lambda^3}} \tag{22}$$

It should be pointed out that the bubble neck diameter d_{neck} changes during the breakup process. In this work, $d_{\text{neck}}=R_1$ was used as the average value for simplification.

To validate Eqs. 18 and 21, the images of bubble breakup reported by Ravelet et al.[34] were used to estimate the times of internal flow and bubble neck shrinking. Image #1906 to image #1914 in Ravelet et al.[34] show the breakup process of a bubble with $d_{\text{neck}}\approx 4.76$ mm. The algorithm proposed by Hermann et al.[55] was used to estimate the radius of curvature. The mean radius of curvature is $R_1\approx 13.8$ mm and $R_2\approx 16.1$ mm for the smaller and larger part of the bubble, respectively. Using these data and Eq. 18, the time t_1 for internal flow is estimated to be 0.290 s. Assuming that the turbulence eddy velocity is 0.3 m/s and using Eq. 21 the time t_2 is estimated to be 0.0258 s. The real time between image #1906 to image #1914 is 0.0267 s, which is very close to t_2 but much smaller than t_1, indicating that the bubble can break up. Other parameters for the calculations were $\zeta_1=0.2$, $\zeta_2=0.3$, $\rho=1.27$ kg/m^3, and $\sigma=0.070$ N/m.

Breakup frequency and daughter bubble/droplet size distribution

The internal flow through the bubble/droplet neck affects both the breakup frequency and daughter size distribution. The bubble/droplet will not breakup when the internal flow is much faster than the neck shrinking. This phenomenon has been experimentally confirmed by Ravelet et al.[34] using high-speed camera. In Figure 14 of their paper, they showed that a bubble did not break up when the internal flow velocity U_{neck} was large because R_1 was much smaller than R_2. By analogy with the probability function for bubble coalescence used by Coulaloglou and Tavlarides,[56] Prince and Blanch[47] and Martin et al.,[57] the following breakup probability function γ was used in this work to account for the effect of internal flow

$$\gamma=\exp\left(-\frac{t_2}{t_1}\right) \tag{23}$$

where t_1 and t_2 are the times for internal flow and neck shrinking, respectively.

The minimum breakup fraction resulted from internal flow through the bubble/droplet neck is obtained by modifying the previous breakup fraction $f_v^{'}$ with the factor γ

$$f_{\text{v,min}}=\gamma f_{\text{v}}^{'} \tag{24}$$

The value of γ is between 0 and 1, indicating that $f_{\text{v,min}}<f_v^{'}$. The possible breakup fraction should between $f_{\text{v,min}}$ and $f_v^{'}$. However, Ravelet et al.[34] reported that a bubble with the shape of Figure 1 may exhibit a large deformation toward equal breakup due to the response of bubble/droplet surface modes to the turbulent forcing.[58,59] Based on this mechanism, the maximum breakup fraction $f_{\text{v,max}}$ was set to be 0.5.

The internal flow through the bubble/droplet affects the overall breakup rate. In this work, the breakup probability function γ was also used as a multiplier to account for this effect. A model assumption that the modified breakup fraction decays by $\exp(-5f_{\text{v}})$ was used. The idea is that the breakup possibility with $f_{\text{v,min}}$ should be large because $f_{\text{v,min}}$ is determined by considering the internal flow, and the turbulent nature of the flow also leads to breakup with $f_v>f_{v,\text{min}}$, but the possibility decreases with increasing f_v. The function $5\exp(-5f_{\text{v}})/[\exp(-5f_{\text{v,min}})-\exp(-5f_{\text{v,max}})]$ was used to describe this trend. Thus, the specific breakup rate of a bubble/droplet with size d breaking with breakup fraction f_{v} can be calculated as

$$\Omega(f_{\text{v}}|d)=\int_{f_{\text{v,min}}}^{f_{\text{v,max}}}\Omega(f_{\text{v}}^{'}|d)\frac{5\gamma\exp(-5f_{\text{v}})}{\exp(-5f_{\text{v,min}})-\exp(-5f_{\text{v,max}})}\mathrm{d}f_{\text{v}}^{'},\quad (f_{\text{v}}\ge f_{\text{v,min}}) \tag{25}$$

The total breakup rate $\Omega(d)$, breakup frequency $b(d)$, and daughter bubble/droplet size distribution $\beta(f_{\text{v}},d)$ are calculated as

$$\Omega(d)=\int_0^{0.5}\Omega(f_{\text{v}}|d)\mathrm{d}f_{\text{v}} \tag{26}$$

$$b(d)=\Omega(d)/n \tag{27}$$

$$\beta(f_{\text{v}},d)=\frac{\Omega(f_{\text{v}}|d)}{\int_0^{0.5}\Omega(f_{\text{v}}|d)\mathrm{d}f_{\text{v}}} \tag{28}$$

Different symbols and names have been used in the literature to describe the bubble breakup. In the paper of Luo and Svendsen,[42] $\Omega_{\text{B}}(v)$ is used for the total breakup rate of particles of size v and has a unit of s^{-1} m^{-3}, and $\Omega/[(1-\varepsilon_{\text{d}})n]$ is used for the specific breakage rate and has a unit of s^{-1}. In a recent paper from Luo's group,[43] $b(v)$ is used for the total breakup rate of particles of size v and $b/[(1-\varepsilon_{\text{d}})n]$ is used for the specific breakage rate. In the paper of Martinez-Bazan et al.[60,61], $g(D)$ is used for the bubble breakup frequency of a bubble with size D and has a unit of s^{-1}. Solsvik et al.[49] point out in their review article that the breakup frequency and total breakage rate are frequently used in an erroneous manner in the literature. They use the symbol b for the bubble breakup frequency and Ω for the total breakup rate, and give a clear discussion of the relationship between these two quantities. To avoid confusion, the symbols and names recommended by Solsvik et al.[49] were used in this work. It should be pointed out that Eq. 27 does not include the number of daughter bubble/droplets as given by Solsvik et al.[49] The reason is that $\Omega(f_v^{'}|d)$ in this work is the specific rate that a bubble/droplet of size d breaks up with a breakup fraction of $f_v^{'}$ while that used by Solsvik et al.[49] is the specific rate that a daughter bubble/droplet of $df_v^{'1/3}$ is produced. For binary breakups, these two definitions differ by a factor of 2, which is the number of daughter bubble/droplets.

Results and Discussion

Model validation and effect of model parameters

Model Validation with Experimental Results. The bubble breakup frequency for mother bubbles of 5, 8, and 10 mm were calculated at different gas densities, as shown in Figure 2.

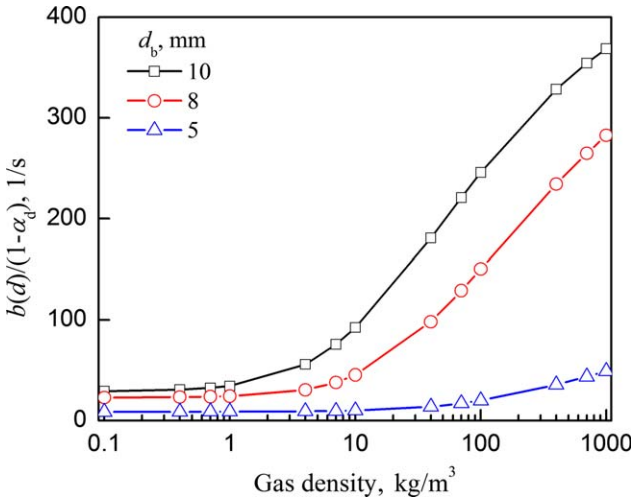

Figure 2. Effect of pressure on the breakup frequency $b(d)$ ($\sigma = 0.072$ N/m, $\varepsilon = 2.0$ m^2/s^3).

[Color figure can be viewed in the online issue, which is available at wileyonlinelibrary.com.]

Because the term $(1 - \alpha_d)$ is unknown, therefore $b(d)/(1 - \alpha_d)$ was used in the figure. The daughter bubble size distributions for $d_b = 10$ mm at different gas densities are shown in Figure 3. Figure 2 shows that the bubble breakup frequency depends on both the bubble size and gas density. When the bubble size is small, the breakup frequency is almost independent of the gas density. However, when the bubble size is large enough, increasing gas density significantly increases the breakup frequency when the gas density exceeds a certain value. The effect of gas density can be divided into two regimes: low density ($\leq$1 kg/m^3) and high density (>1 kg/m^3). In the low-density regime, the breakup frequency is almost independent of the gas density. While in the high-density regime, the breakup frequency significantly increases with increasing gas density.

The model calculations were compared with the experimental data reported by Wilkinson et al.,[28] who performed the bubble breakup experiments in a vertical turbulent flow pipe for different types of gas. For each gas, at least 150 bubbles were injected to evaluate the bubble breakup percentage using a high-speed camera. The experimental data were given in terms of bubble breakup percentage instead of bubble breakup frequency. According to Wilkinson et al.[28] and Maass et al.[62] the bubble breakup percentage q_b is defined as

$$q_b = N_b/N_0 \tag{29}$$

where N_b is number of breaking bubbles, and N_0 is the number of injected bubbles. The breakup frequency $\Omega(d)$ is written as[62]

$$\Omega(d) = q_b/t_b \tag{30}$$

where the bubble breakage time t_b is the time that is needed to breakup an initially deformed bubble, and is a function of the mother bubble diameter d_b and turbulent energy dissipation rate ε.[62] Using Eq. 30, the breakage time t_b at ambient pressure was calculated from the experimental data of bubble breakup percentage q_b in the literature[28] and the predicted breakup frequency using the model of this work, as listed in Table 1. The calculated values of t_b were in the range of 10−100 ms reported by Hesketh et al.[36] From Table 1, it can been seen that the breakage time significantly decreased with increasing bubble size and finally reaches its minimum value. With the assumption that the breakage time is independent of gas density, the predicted bubble breakup percentage q_b is calculated by Eq. 30 for other gas densities, and compared to the experimental data of Wilkinson et al.[28] Figure 4 shows that for different mother bubble sizes the calculated bubble breakup percentages agreed well with the experimental values. The nonlinear effects of both the gas

Table 1. Breakage Time for a Bubble in Ambient Pressure

Bubble Diameter, mm	4.6	5.8	8.3	9.8
Breakage Time, ms	29.5	19.6	14.8	14.6

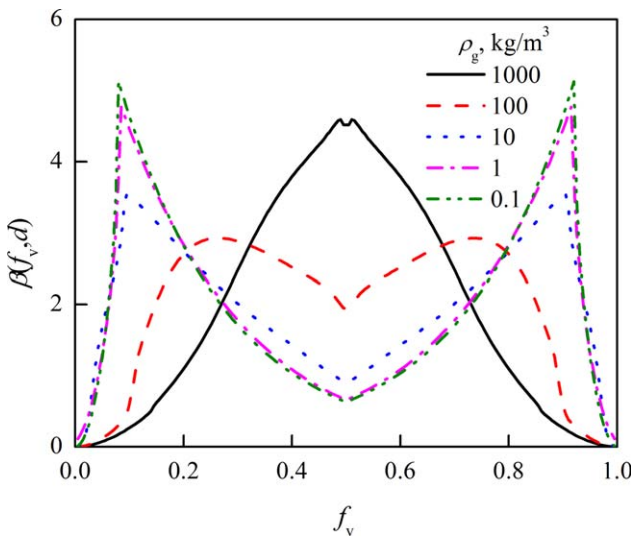

Figure 3. Effect of pressure on the daughter size distribution ($R = 0.005$ m, $\sigma = 0.072$ N/m, $\varepsilon = 2.0$ m^2/s^3).

[Color figure can be viewed in the online issue, which is available at wileyonlinelibrary.com.]

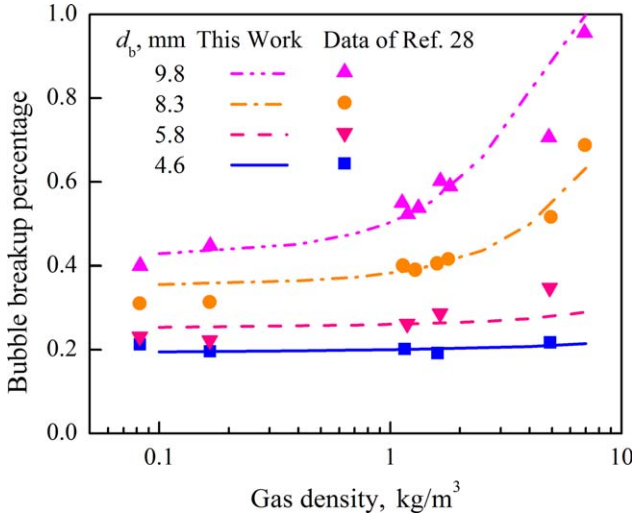

Figure 4. Comparison of the predicted breakup percentage for different mother bubble sizes with the experimental data ($\sigma = 0.072$ N/m, $\varepsilon = 2.0$ m^2/s^3).

[Color figure can be viewed in the online issue, which is available at wileyonlinelibrary.com.]

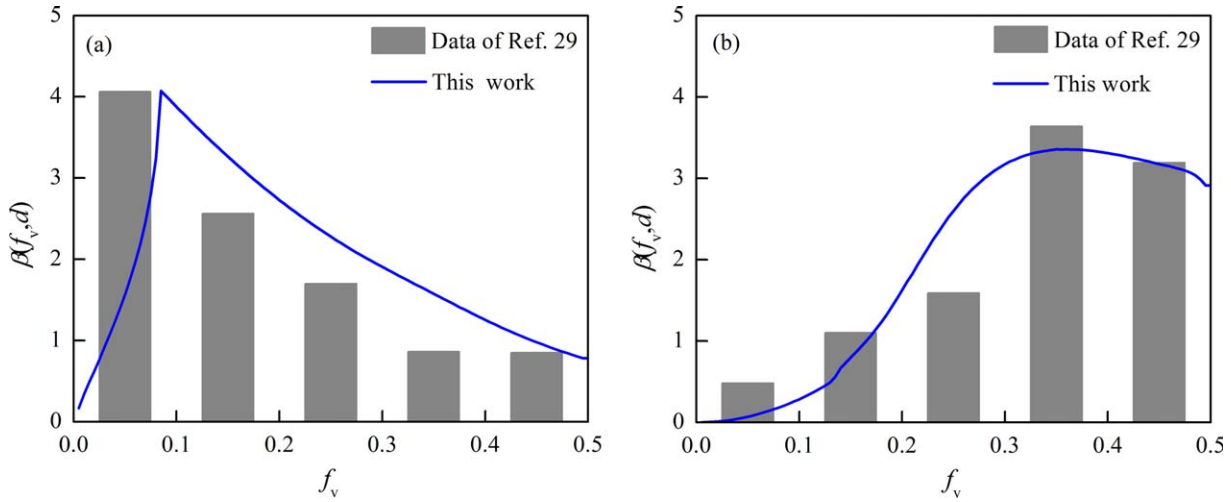

Figure 5. Comparison of the predicted volume-based daughter size distributions by this work with the experimental data.

(a) gas bubble (air-water system, $\rho = 1$ kg/m^3, $R = 0.004$ m, $\sigma = 0.072$ N/m, $\varepsilon = 8.5$ m^2/s^3); (b) liquid droplet (dodecane-water system, $\rho = 750$ kg/m^3, $R = 0.002$ m, $\sigma = 0.053$ N/m, $\varepsilon = 8.5$ m^2/s^3). [Color figure can be viewed in the online issue, which is available at wileyonlinelibrary.com.]

density and bubble size on the bubble breakup are well predicted.

The effect of gas density on the daughter bubble size distribution was also investigated. In low-density regime, the effect of gas density is negligible. While in high-density regime, increasing gas density favors the equal-size breakup. In this case, the daughter size distribution is typically Λ-shaped. Because the gas density increases with increasing pressure, the extreme case is that a gas bubble becomes a liquid droplet when the gas density is ~1000 kg/m^3. The calculated daughter bubble/droplet size distributions are comparable to the experimental data of Andersson and Andersson for both bubbles and droplets,[29] as shown in Figure 5. Experimental results show that at moderate energy dissipation rate, bubbles often break into unequal size fragments while droplets tend to break into equal-size fragments. However, different results have been reported under other conditions. For example, Martinez-Bazan et al.[60,61] found by experiments that at a very high energy dissipation rate ($\varepsilon = 1000$ m^2/s^3) bubbles tend to breakup into daughter bubbles of similar size. Thus, bubbles have an M-shape daughter bubble size distribution while droplets have a Λ-shape daughter droplet size distribution.[29,36,37,63] To our best knowledge, none of the reported breakup models can predict the different daughter size distribution of bubbles and droplets. The model of Luo and Svendsen,[42] Lehr et al.,[64] Wang et al.,[41] and Zhao and Ge[35] show an M-shape or U-shape bubble size distribution for both bubble and droplet breakup, while the models of Martinez-Bazan et al.[61] and Han et al.[43] show a Λ-shape. The unified model proposed in this work shows good predictions of both bubbles and droplets.

In this work, if the effect of internal flow is not considered, the bubble breakup rate will be independent of the pressure or gas density, and the daughter bubble size distribution will usually show a "Λ" shape. When the effect of the internal flow is considered, the breakup behaviors that the bubble breakup rate increases with increasing pressure or gas density and the daughter bubble size distribution is usually shown an "M" shape while the daughter droplet size distribution usually has a "Λ" shape are correctly predicted. As a result, the unified model proposed in this work shows good predictions of both bubble and droplet breakup behaviors.

Effect of Model Parameters. Because the effects of pressure on both gas and liquid viscosity are very small,[65,66] they were not considered in this work. The effect of pressure is more significant on surface tension than on viscosity.[67] For example, the relative surface tension for the ethylene-water system decreased from 1.0 to 0.7 when the pressure increased from 0 to 40 atm.[67] For simplification, the effect of pressure on surface tension was also not considered in this calculations. Nevertheless, the effect of pressure on surface tension and viscosity can be easily included in the calculations using the values at a given condition.

The Kolmogorov microscale of eddies, $\eta_{e,K}$, should be used as the lower limit, but it has been replaced by the minimum size of eddies in the inertial subrange of isotropic turbulence, λ_{min}. The reason is that the expressions for bombarding frequency of eddies and breakage probability developed earlier are only valid for this subrange. This change is acceptable as the very small eddies have very low energy contents and very short lifetimes, thereby having a negligible effect on the breakage of particles. Tennekes and Lumley[68] have given the minimum size of eddies in the inertia subrange as $2\pi\eta_{e,K}/\lambda_{min} = 0.2$–$0.55$ or $\lambda_{min}/\eta_{e,K} = 11.4$–$31.4$. The value $2\pi\eta_{e,K}/\lambda_{min} = 0.55$ is determined by requiring that the integral of dissipation spectra is equal to the dissipation rate ε. At this point, $E(\kappa)$ can be approximated by $\alpha\varepsilon^{2/3}\kappa^{-3/5}$ but with a slight deviation. At the value of $2\pi\eta_{e,K}/\lambda_{min} = 0.2$, $D(\kappa)$ has its peak value and $E(\kappa)$ has very small deviation from $\alpha\varepsilon^{2/3}\kappa^{-3/5}$. Thus, when $\lambda_{min}/\eta_{e,K} = 11.4$ or $2\pi\eta_{e,K}/\lambda_{min} = 0.55$ is used as the limit, $E(\kappa) = \alpha\varepsilon^{2/3}\kappa^{-3/5}$ is approximately satisfied; when $\lambda_{min}/\eta_{e,K} = 31.4$ or $2\pi\eta_{e,K}/\lambda_{min} = 0.2$ is used, $E(\kappa) = \alpha\varepsilon^{2/3}\kappa^{-3/5}$ is satisfied more strictly. The effect of the λ_{min} value on the bubble breakup frequency has been discussed in our previous work.[41] For a bubble size $d = 3$ mm and turbulent energy dissipation rate $\varepsilon = 1.0$ m^2/s^3 in air-water system, the Kolmogorov length $\lambda_d = \nu^{3/4}/\varepsilon^{1/4} = 3.2 \times 10^{-5}$ m, and the mean kinetic energy of an eddy of size 31.4 times λ_d is 7.1×10^{-7} J. However, the increase in surface energy is to 5.2×10^{-7} J for equal

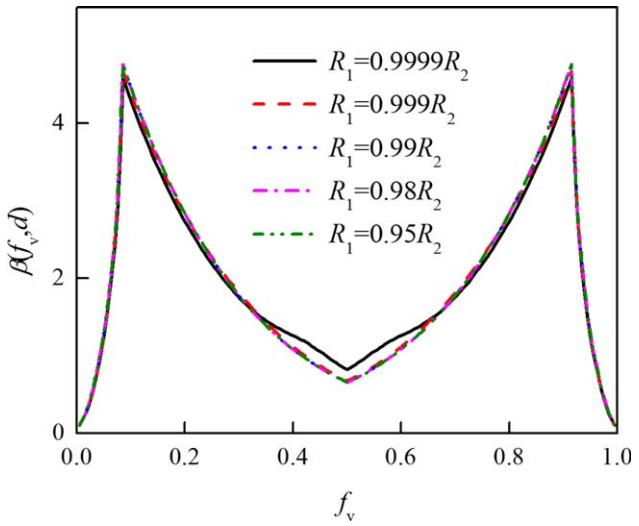

Figure 6. Effect of δ for the specific initial condition of $R_1 = R_2$ on the daughter size distribution ($R = 0.005$ m, $\rho = 1$ kg/m^3, $\sigma = 0.072$ N/m, $\varepsilon = 2.0$ m^2/s^3).

[Color figure can be viewed in the online issue, which is available at wileyonlinelibrary.com.]

breakup of a bubble with size 3 mm. Therefore, most small eddies in the viscous subrange cannot satisfy the bubble breakup constraints and have almost no effect on the bubble breakup.

We checked the effect of the upper limit of integral on the breakup frequency for $\sigma = 0.072$N/m, $\varepsilon = 2.0$ m^2/s^3, ρ =1, and 100 kg/m^3. The results showed that the breakup frequency was about 20% larger with $\lambda_{max}/d_b = 2$ than with $\lambda_{max}/d_b = 1$, and became almost independent of λ_{max}/d_b when $\lambda_{max}/d_b > 2$. Therefore, $\lambda_{max}/d_b = 3$ was used in this work. Han et al.[43] have reported similar results that the eddies with size $\lambda > 5d_b$ have little contribution to the overall breakup frequency, and those with size $\lambda \leq 3d_b$ contribute to most of the overall breakup frequency.

It should be pointed out that when the initial values of R_1 and R_2 are equal, the pressures inside the two parts of the bubble are equal and the internal flow cannot be initialized. For this specific case, the function $\exp(-5f_v)/[\exp(-5f_{v,min})-\exp(-5f_{v,max})]$ has no meaning because $f_{v,min} = f_{v,max} = 0.5$. In the real gas-liquid flow, however, the random nature of turbulence will exert perturbations to the deformed bubbles with two equal-size parts and result in a small difference between R_1 and R_2. To account for this effect, a small difference was set between R_1 and R_2, that is, $R_1 = (1-\delta)R_2$, for the case of $R_1 = R_2$. Although the value of δ has a much larger effect on the time scale t_1, it has negligible effect on the daughter size distribution. The calculated daughter size distributions with different values of δ are shown in Figure 6. It can be seen that the daughter size distribution is independent of δ when δ is between 0.05 and 0.001. Only with a very small value of $\delta = 0.0001$, the calculated daughter size distributions have slightly larger values near $f_v = 0{,}5$. This is an expected result because the case of $R_1 = R_2$ ($f_v = 0.5$) is only one point in the integral range of $f_{v,min}$ of Eq. 25. In this work, $R_1 = 0.98R_2$ was used for the case of $R_1 = R_2$ in all calculations. Note that this treatment was only used for the specific case of $R_1 = R_2$.

During the breakup process, R_1, R_2, U_{neck}, and d_{neck} all change with time. This makes the breakup process very complex and difficult to describe accurately. In this model, the variations of these parameters were not considered when estimating the time scale. The validity of this simplification was checked by numerical integration of the differential form of Eq. 18 so that the changes of R_1, R_2, U_{neck}, and d_{neck} could be considered. For $R = 0.002$ m, $\rho = 1$ kg/m^3, and $\sigma = 0.072$ N/m, the value of t_1 calculated by numerical integration is close to that by Eq. 18, confirming that Eq. 18 is a reasonable simplification to calculate the time t_1.

Equation 18 is a simplified calculation of t_1 because the effect of variations of R_1, R_2, and U_{neck} was not considered. To check the validity of this simplification, the following differential equation was used to calculate the time t_1 to account for the time variation of R_1, R_2, and U_{neck}

$$dt_1 = \frac{1}{U_{neck}\pi d_{neck}^2/4} dV_1 = \frac{8}{\sqrt{\frac{\sigma}{(\zeta_1+\zeta_2)\rho}\left(\frac{1}{R_1} - \frac{1}{\sqrt[3]{R^3 - R_1^3}}\right)} dR_1} \quad (31)$$

The time scale t_1 considering the variation of R_1, R_2, and U_{neck} was calculated by integration of Eq. 31 numerically, and the result was called $t_{1,varied}$. The calculation results for $R = 0.002$ m, $\rho = 1$ kg/m^3, and $\sigma = 0.072$ N/m show that $t_{1,average}$ is close to $t_{1,varied}$ and the daughter size distribution using $t_{1,average}$ and $t_{1,varied}$ are very similar. Considering that the numerical integration of Eq. 31 makes the calculation of the breakup model very time-consuming, and $t_{1,average}$ is a good approximation of $t_{1,varied}$, the simplified calculation using Eq. 18 was used in this work.

This model is relatively time consuming because multiple integrals are involved, with a computational cost similar to our previous model.[41] Further improvement can be made to accelerate the calculation. For example, we developed an algorithm to reduce the triple integral in our previous bubble/droplet breakup model to double integral.[69]

Breakup frequency

Effect of Mother Bubble/Droplet Diameter. Figure 7 shows the effect of the mother bubble diameter on the breakup frequency at different gas densities. It can be seen

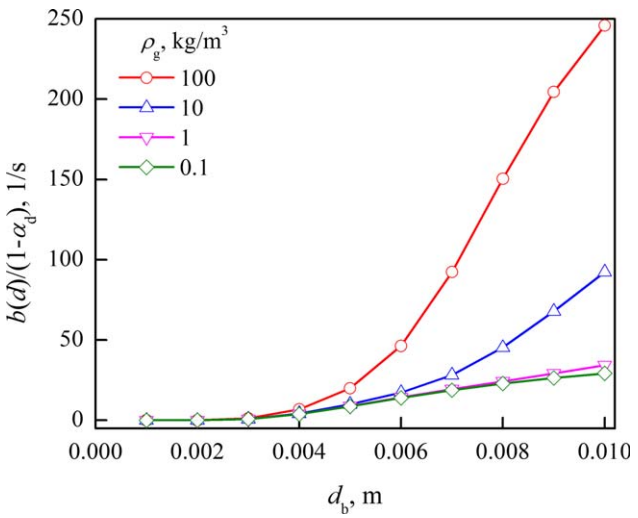

Figure 7. Effect of the mother diameter on the breakup frequency $b(d)$ at different gas densities ($\sigma = 0.072$ N/m, $\varepsilon = 2.0$ m^2/s^3).

[Color figure can be viewed in the online issue, which is available at wileyonlinelibrary.com.]

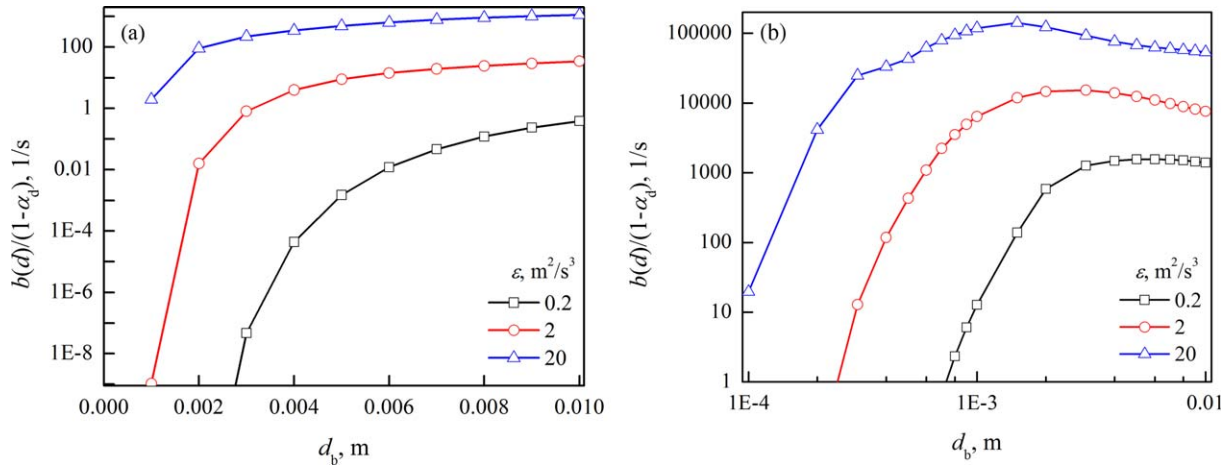

Figure 8. Effect of energy dissipation rate on the breakup frequency *b*(*d*).

(a) Gas bubble (air-water system, $\sigma = 0.072$N/m, $\rho = 1$ kg/m^3); (b) liquid droplet (oil-water system, $\sigma = 0.002$ N/m, $\rho = 760$ kg/m^3). [Color figure can be viewed in the online issue, which is available at wileyonlinelibrary.com.]

that the calculated bubble breakup frequency increases with increasing mother bubble diameter. This is consistent with the results in the literature.[35,41,43,44] In the full range of gas densities, the bubble breakup frequency is very small in low to moderate turbulent energy dissipation rate when the mother bubble is smaller than ~3 mm, indicating that small bubbles can hardly breakup. This is because small bubbles have rigid surface and the internal flow through the neck is fast. The breakup frequency increases with increasing mother bubble diameter, and this effect becomes less significant with a further increase in the mother bubble diameter. The breakup frequency depends on both the collision frequency ϖ_λ(d) and the probability density function $P_b(f_v^{'}|d,\lambda)$. Equations 2 and 4 show that ϖ_λ (d) increases and $P_b(f_v^{'}|d,\lambda)$ decreases with increasing mother droplet diameter. The variation of the breakup frequency with the mother droplet diameter is determined by the extent of these two effects. For some cases, the breakup frequency peaks at a center droplet diameter and then levels out, and in some cases even decreases, which is consistent with the experimental results of Maass et al.[62]

Effect of Turbulent Energy Dissipation Rate. The turbulent energy dissipation rate, which is the most important parameter of a turbulent flow, determines the number density and energy distribution of the turbulent eddies. The increase in the turbulent energy dissipation rate increases both the collision frequency between eddies and bubbles/droplets and the kinetic energy contained in eddies, therefore increases the bubble/droplet breakup frequency, as shown in Figure 8. Increasing the energy dissipation rate by one order of magnitude causes an increase of about two orders of magnitude in the breakup frequency. This suggests that increasing the turbulence intensity is an effective approach to enhance bubble breakup.

Effect of Surface Tension. Figure 9 shows the effect of surface tension on the breakup frequency. Decreasing surface tension significantly increases the breakup frequency for both bubbles and droplets, especially in the low surface tension range. Because the surface tension of organic liquid is usually in the range of 0.02−0.03 N/m, which is much lower than that of water (0.072 N/m), the breakup frequency of bubbles/droplets in organic fluid is much larger, which leads

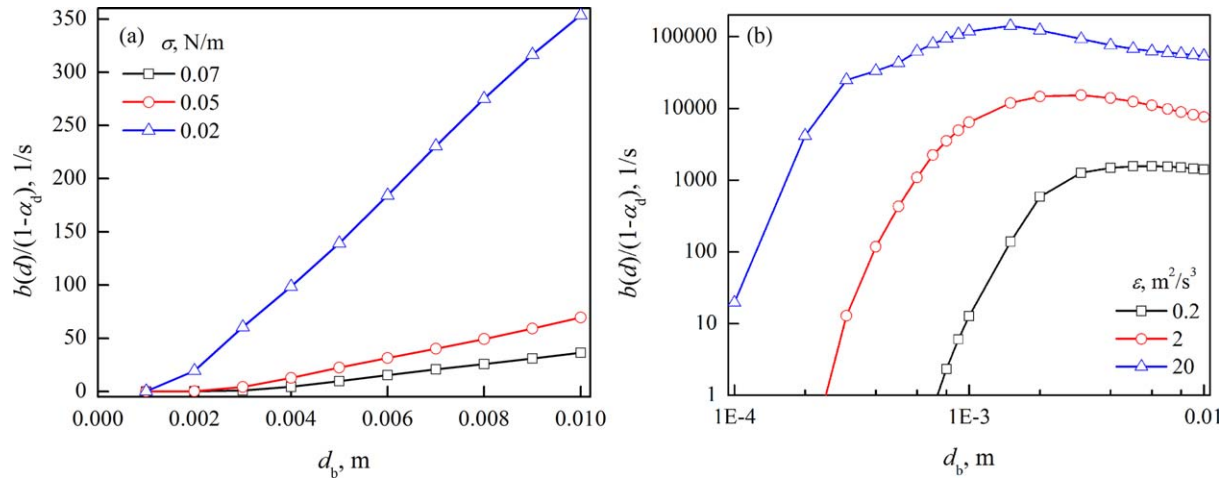

Figure 9. Effect of surface tension on the breakup frequency *b*(*d*).

(a) Gas bubble ($\rho = 1$ kg/m^3, $\varepsilon = 2.0$ m^2/s^3); (b) liquid droplet (oil-water system, $\rho = 760$ kg/m^3, $\varepsilon = 2.0$ m^2/s^3). [Color figure can be viewed in the online issue, which is available at wileyonlinelibrary.com.]

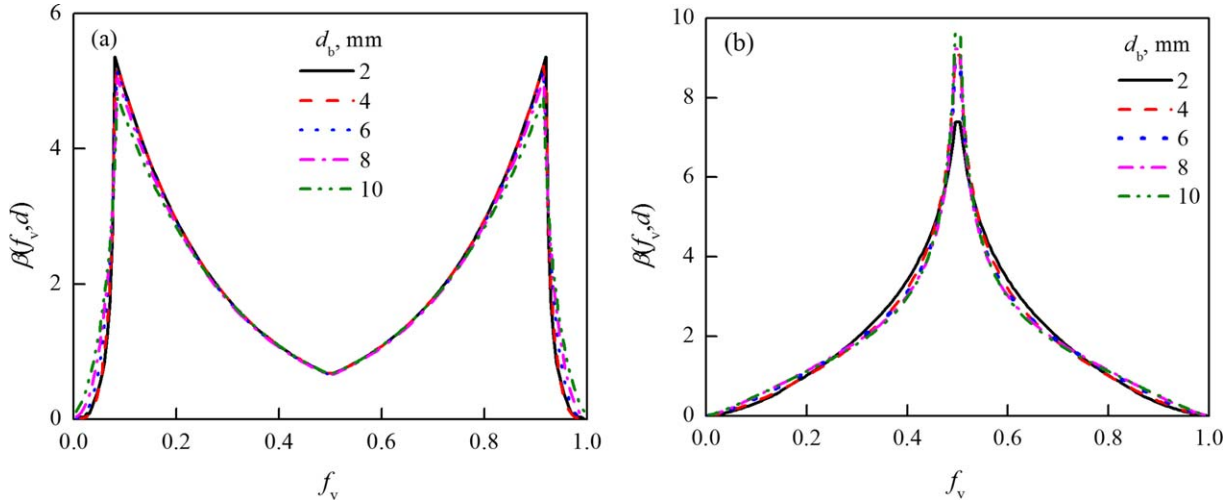

Figure 10. Effect of mother diameter on the daughter size distribution.

(a) Gas bubble ($\sigma = 0.072$ N/m, $\rho = 1$ kg/m^3, $\varepsilon = 2.0$ m^2/s^3); (b) liquid droplet (oil-water system, $\sigma = 0.002$ N/m, $\rho = 760$ kg/m^3, $\varepsilon = 2.0$ m^2/s^3). [Color figure can be viewed in the online issue, which is available at wileyonlinelibrary.com.]

to smaller bubble size. For a liquid-liquid system, the surface tension will be much lower than a gas-liquid system. For example, the typical surface tension for the water-octane-surfactant system varied from about 10^{-3} to 10^{-7} N/m.[70] This explains that when the system are added or polluted with surfactants, the droplet breakup frequency is very large and very small droplets can also break up. The above discussion gives a better understanding and some quantitative analysis of the phenomenon that the gas holdup significantly increases with the addition of surfactants or decreasing surface tension, which have been widely reported in the literature.[16,71,72]

Daughter bubble/droplet size distribution

Effect of Mother Bubble/Droplet Diameter. The effect of mother bubble/droplet diameter on the daughter size distribution are shown in Figure 10. For bubbles and droplets, the daughter size distribution is nearly independent of the mother diameter at typical surface tension and moderate energy dissipation rate, and the equal-size breakup only slightly increases with increasing mother diameter. But at a very high energy dissipation rate, the effect of the mother bubble diameter is significant, and equal-size breakup was predicted at $\varepsilon = 1000$ m^2/s^3. The existing breakup models have predicted different effects of the mother diameter on the daughter size distribution. The models of Martinez-Bazan et al.,[61] Lehr et al.,[64] and Wang et al.[41] predict that increasing mother size increases the probability of equal-size breakup while the models of Luo and Svendsen,[42] Zhao and Ge[35] predict the opposite trend. Due to lack of experimental data and different conditions investigated, it is hard to determine which trend is correct. More experiments are needed to fully validate the model and guide further model improvement. Bubbles exhibit an M-shaped daughter bubble size distribution and droplets have a Λ-shaped daughter size distribution. When the mother bubble/droplet diameter is large enough, the equal-size breakup is slightly enhanced with increasing diameter.

Effect of Turbulent Energy Dissipation Rate. The turbulent energy dissipation rate has significant effects on the

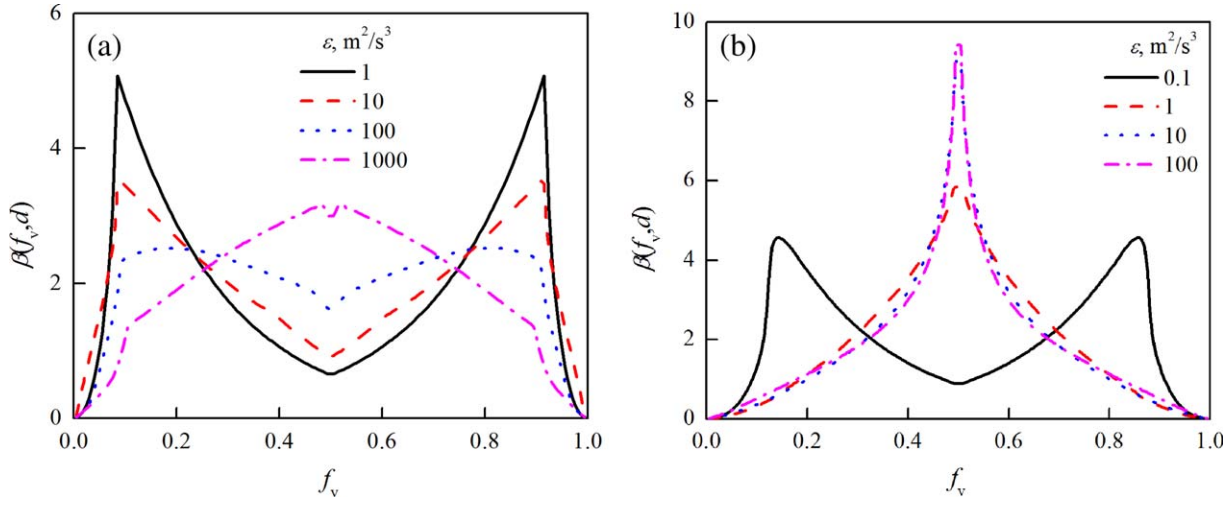

Figure 11. Effect of turbulent energy dissipation rate on the daughter size distribution.

(a) Gas bubble ($R = 0.005$ m, $\rho = 1$ kg/m^3, $\sigma = 0.072$ N/m); (b) liquid droplet (oil-water system, $R = 0.001$ m, $\rho = 760$ kg/m^3, $\sigma = 0.002$ N/m). [Color figure can be viewed in the online issue, which is available at wileyonlinelibrary.com.]

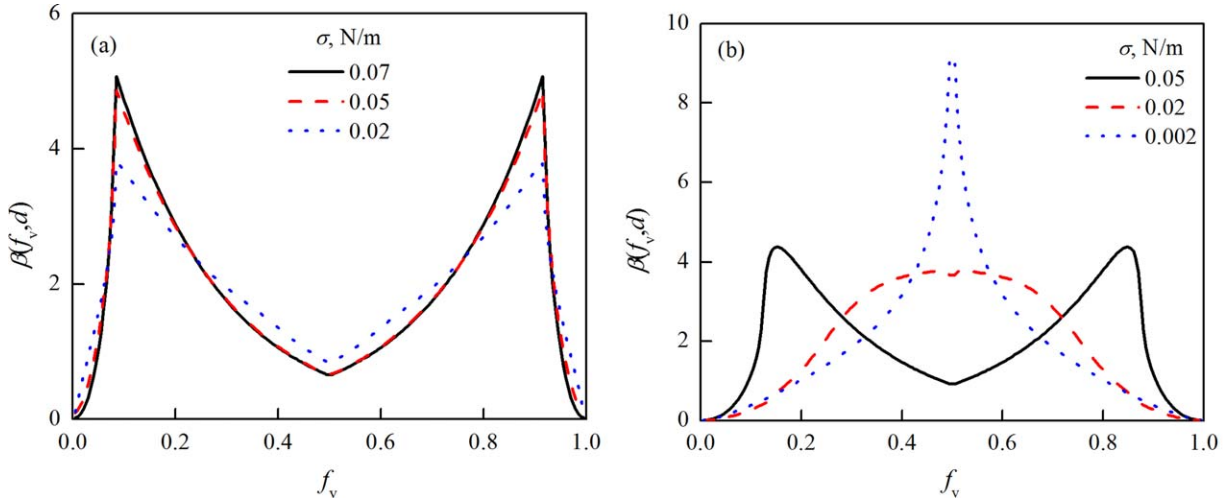

Figure 12. Effect of surface tension on the daughter size distribution (a) bubble breakup ($R = 0.005$ m, $\rho = 1$ kg/m^3, $\varepsilon = 1.0$ m^2/s^3); (b) droplet breakup (oil-water system, $R = 0.002$ m, $\rho = 760$ kg/m^3, $\varepsilon = 2.5$ m^2/s^3).

[Color figure can be viewed in the online issue, which is available at wileyonlinelibrary.com.]

daughter bubble/droplet size distribution, as shown in Figure 11. The equal breakup probability increases with increasing turbulent energy dissipation rate, and at $\varepsilon = 1000$ m^2/s^3 the bubbles tend to breakup in equal-size fragments. Different from the existing breakup models, this model successfully predicts both the equal and unequal daughter size distribution observed at different conditions. In contrast, droplets show different types of daughter size distribution in a wide range of turbulent energy dissipation rate. At very low turbulent energy dissipate rate, the daughter droplet size distribution has an M shape, while for medium and high turbulent energy dissipation rate, it has a "Λ" shape. When the turbulent energy dissipation rate is beyond a certain value, a further increase of turbulent energy dissipation rate has negligible effect on the daughter droplet size distribution.

Effect of Surface Tension. Figure 12 shows the effect of surface tension on the daughter bubble/droplet size distribution. For bubble breakup, the daughter bubble size distribution is not sensitive to surface tension. The general trend is that the probability of equal breakup slightly increases with decreasing surface tension when the surface tension is lower than a certain value. For droplet breakup calculations, the parameters of a typical oil-water system ($\rho = 760$ kg/m^3, $\varepsilon = 2.5$ m^2/s^3, $\sigma = 0.002$ N/m) are used.[37] The results show that the daughter droplet size distribution is more sensitive to surface tension than bubbles. In the low to medium surface tension range, the droplet size distribution has a "Λ" shape while at very large surface tension the droplet size distribution has an "M" shape. These complex breakup behaviors predicted by the breakup model need further experimental validation.

Conclusions

The internal flow through the bubble/droplet neck during the deformation and breakup process was analyzed based on the Young–Laplace equation and the Bernoulli equation, and was further included in the unified breakup model for both bubbles and droplets. Two time scales, that is, the time t_1 for the smaller part completely flow into the larger part of a deformed bubble/droplet, and the time t_2 for shrinking of the bubble/droplet neck till collapse, were proposed to quantitatively describe the effect of the internal flow through the bubble/droplet neck on the breakup frequency and daughter bubble/droplet size distribution. The internal flow behavior strongly depended on the gas density or pressure, and based on this mechanism, the effects of pressure on the breakup behavior and bubble size distribution were well understood. For the first time, this unified breakup model gave good predictions of the effect of gas density on bubble breakup frequency and the different breakup behaviors of bubbles and droplets. With this model, the effect of the mother bubble/droplet diameter, turbulent energy dissipation rate and surface tension on the breakup frequency, and daughter bubble/droplet size distribution were discussed. Further work will focus on the evaluation and exploration of the new bubble breakup model in a PBM to investigate the effect of pressure on the bubble size distribution and coupling CFD simulations with PBM to study the effect of pressure on the hydrodynamic behaviors of a bubble column.

Acknowledgment

The authors gratefully acknowledge the financial supports by the National Natural Science Foundation of China (No. 21476122) and Program for New Century Excellent Talents in University (NCET-12-0297).

Notation

$b(d)$ = breakup frequency, s^{-1}
c_f = parameter of increase of surface energy, –
c_d = parameter of increase of surface energy per unit volume, –
d_b = diameter of the mother bubble, m
d_λ = diameter of the turbulent eddy, m
d_{neck} = diameter of the bubble/droplet neck, m
$e(\lambda)$ = kinetic energy of an eddy with size λ, J
k_{neck} = ratio of the bubble/droplet neck to the smaller fragment, –
l_{neck} = length of the bubble/droplet neck, m
n = number density of bubble/droplet with size d, m^{-3}
n_λ = number density function of turbulent eddies with size λ, m^{-4}
N_b = number of breaking bubbles t_b seconds after the bubble injection, –
N_0 = number of injected bubbles, –
P = pressure, Pa
$P_b(f_v'|d,\lambda)$ = breakup probability density for a bubble with size d breaking with breakup fraction f_v' when hit by an eddy of size λ, –
q_b = bubble breakup percentage, –
R = radius, m

Re = Reynolds number, –
t_1 = the time scale for the smaller part completely flows into the larger part, s
t_2 = the time scale for the shrinking bubble neck to cut off, s
t_b = breakage time for a bubble in ambient pressure, s
U_λ = turbulent velocity of an eddy with size λ, m s^{-1}
U_{neck} = internal gas flow velocity, m s^{-1}
U_{plus} = additional shrinking velocity, m s^{-1}
$\bar{u}$ = the mean turbulent velocity at a distance of d_b, m s^{-1}
$\bar{u}_\lambda$ = mean turbulent velocity of an eddy with size λ, m s^{-1}
V_1 = volume of smaller part of the deformed bubble, m^3

Greek letters

α = phase holdup, –
$\beta(f_v,d)$ = daughter size distribution
ε = energy dissipation rate, m^2 s^{-3}
γ = the breakup probability function γ of the bubble/droplet neck, –
κ = the friction coefficient, –
λ = eddy size, m
λ_{min} = minimum eddy size effective for breakup, m
μ = viscosity, mPa s
ρ = density, kg m^{-3}
σ = surface tension, N m^{-1}
τ_e = turbulenct eddy life time, s
$\varpi_\lambda(d)$ = collision frequency density of eddies with size between λ and $\lambda + d\lambda$ and bubbles with size d, m^{-5} s^{-1}
Ω = total breakup rate, m^{-3} s^{-1}
ξ = ratio of the eddy size λ to the bubble/droplet size d_b, –
ζ_1 = minor loss coefficient of contraction, –
ζ_2 = minor loss coefficient of expansion, –

Literature Cited

1. Wilkinson PM, Vondierendonck LL. Pressure and gas-density effects on bubble break-up and gas hold-up in bubble-columns. *Chem Eng Sci*. 1990;45(8):2309–2315.
2. Letzel HM, Schouten JC, van den Bleek CM, Krishna R. Influence of elevated pressure on the stability of bubbly flows. *Chem Eng Sci*. 1997;52(21–22):3733–3739.
3. Luo XK, Lee DJ, Lau R, Yang GQ, Fan LS. Maximum stable bubble size and gas holdup in high-pressure slurry bubble columns. *AIChE J*. 1999;45(4):665–680.
4. Yang GQ, Fan LS. Axial liquid mixing in high-pressure bubble columns. *AIChE J*. 2003;49(8):1995–2008.
5. Rudkevitch D, Macchi A. Hydrodynamics of a high pressure three-phase fluidized bed subject to foaming. *Can J Chem Eng*. 2008; 86(3):293–301.
6. Krishna R, Deswart JWA, Hennephof DE, Ellenberger J, Hoefsloot HCJ. Influence of increased gas density on the hydrodynamics of bubble column reactors. *AIChE J*. 1994;40(1):112–119.
7. Macchi A, Bi H, Grace JR, McKnight CA, Hackman L. Effect of gas density on the hydrodynamics of bubble columns and three-phase fluidized beds. *Can J Chem Eng*. 2003;81(3–4):846–852.
8. Strasser W, Wonders A. Hydrokinetic optimization of commercial scale slurry bubble column reactor. *AIChE J*. 2012;58(3):946–956.
9. Stegeman D, Knop PA, Wijnands AJG, Westerterp KR. Interfacial area and gas holdup in a bubble column reactor at elevated pressures. *Ind Eng Chem Res*. 1996;35(11):3842–3847.
10. Letzel HM, Schouten JC, Krishna R, van den Bleek CM. Gas holdup and mass transfer in bubble column reactors operated at elevated pressure. *Chem Eng Sci*. 1999;54(13–14):2237–2246.
11. Urseanu MI, Guit RPM, Stankiewicz A, van Kranenburg G, Lommen J. Influence of operating pressure on the gas hold-up in bubble columns for high viscous media. *Chem Eng Sci*. 2003;58(3–6):697–704.
12. Chilekar VP, van der Schaaf J, Kuster BFM, Tinge JT, Schouten JC. Influence of elevated pressure and particle lyophobicity on hydrodynamics and gas-liquid mass transfer in slurry bubble columns. *AIChE J*. 2010;56(3):584–596.
13. Behkish A, Lemoine R, Sehabiague L, Oukaci R, Morsi BI. Gas holdup and bubble size behavior in a large-scale slurry bubble column reactor operating with an organic liquid under elevated pressures and temperatures. *Chem Eng J*. 2007;128(2–3):69–84.
14. Kemoun A, Ong BC, Gupta P, Al-Dahhan MH, Dudukovic MP. Gas holdup in bubble columns at elevated pressure via computed tomography. *Int J Multiphase Flow*. 2001;27(5):929–946.
15. Deckwer WD, Schumpe A. Improved tools for bubble column reactor design and scale-up. *Chem Eng Sci*. 1993;48(5):889–911.
16. Krishna R, Wilkinson PM, Vandierendonck LL. A model for gas holdup in bubble columns incorporating the influence of gas density on flow regime transitions. *Chem Eng Sci*. 1991;46(10):2491–2496.
17. Letzel MH. Effect of gas density on large-bubble holdup in bubble column reactors. *AIChE J*. 1998;44(10):2333–2336.
18. Dewes I, Schumpe A. Gas density effect on mass transfer in the slurry bubble column. *Chem Eng Sci*. 1997;52(21–22):4105–4109.
19. Jin HB, Yang SH, Zhang TW, Tong ZM. Bubble behavior of a large-scale bubble column with elevated pressure. *Chem Eng Technol*. 2004;27(9):1007–1013.
20. Jordan U, Saxena AK, Schumpe A. Dynamic gas disengagement in a high-pressure bubble column. *Can J Chem Eng*. 2003;81(3–4): 491–498.
21. Fan LS, Yang GQ, Lee DJ, Tsuchiya K, Luo X. Some aspects of high-pressure phenomena of bubbles in liquids and liquid-solid suspensions. *Chem Eng Sci*. 1999;54(21):4681–4709.
22. Zhang JP, Li Y, Fan LS. Numerical studies of bubble and particle dynamics in a three-phase fluidized bed at elevated pressures. *Powder Technol*. 2000;112(1–2):46–56.
23. Keim NC. Perturbed breakup of gas bubbles in water: memory, gas flow, and coalescence. *Phys Rev E*. 2011;83(5):056325.
24. Li BB, Zhang HC, Lu J, Ni XW. Experimental investigation of the effect of ambient pressure on laser-induced bubble dynamics. *Opt Laser Technol*. 2011;43(8):1499–1503.
25. Sagert NH, Quinn MJ. Coalescence of H2S and CO2 bubbles in water. *Can J Chem Eng*. 1976;54(5):392–398.
26. Sagert NH, Quinn MJ. Influence of high-pressure gases on stability of thin aqueous films. *J Colloid Interface Sci*. 1977;61(2):279–286.
27. Lin TJ, Tsuchiya K, Fan LS. Bubble flow characteristics in bubble columns at elevated pressure and temperature. *AIChE J*. 1998;44(3): 545–560.
28. Wilkinson PM, Vanschayk A, Spronken JPM, Vandierendonck LL. The influence of gas-density and liquid properties on bubble breakup. *Chem Eng Sci*. 1993;48(7):1213–1226.
29. Andersson R, Andersson B. On the breakup of fluid particles in turbulent flows. *AIChE J*. 2006;52(6):2020–2030.
30. Quan SP, Hua JS. Numerical studies of bubble necking in viscous liquids. *Phys Rev E*. 2008;77(6):066303.
31. Bergmann R, van der Meer D, Stijnman M, Sandtke M, Prosperetti A, Lohse D. Giant bubble pinch-off. *Phys Rev Lett*. 2006;96(15): 154505.
32. Gordillo JM, Perez-Saborid M. Axisymmetric breakup of bubbles at high Reynolds numbers. *J Fluid Mech*. 2006;562:303–312.
33. Thoroddsen ST, Etoh TG, Takehara K. Experiments on bubble pinch-off. *Phys Fluids*. 2007;19(4):042101.
34. Ravelet F, Colin C, Risso F. On the dynamics and breakup of a bubble rising in a turbulent flow. *Phys Fluids*. 2011;23(10):103301.
35. Zhao H, Ge W. A theoretical bubble breakup model for slurry beds or three-phase fluidized beds under high pressure. *Chem Eng Sci*. 2007;62(1–2):109–115.
36. Hesketh RP, Etchells AW, Russell TWF. Experimental observations of bubble breakage in turbulent. *Ind Eng Chem Res*. 1991;30(5): 835–841.
37. Zaccone A, Gaebler A, Maass S, Marchisio D, Kraume M. Drop breakage in liquid-liquid stirred dispersions: modelling of single drop breakage. *Chem Eng Sci*. 2007;62(22):6297–6307.
38. Wang TF, Wang JF, Jin Y. Population balance model for gas-liquid flows: influence of bubble coalescence and breakup models. *Ind Eng Chem Res*. 2005;44(19):7540–7549.
39. Xing CT, Wang TF, Wang JF. Experimental study and numerical simulation with a coupled CFD-PBM model of the effect of liquid viscosity in a bubble column. *Chem Eng Sci*. 2013;95:313–322.
40. Wang TF, Wang JF, Jin Y. A CFD-PBM coupled model for gas-liquid flows. *AIChE J*. 2006;52(1):125–140.
41. Wang TF, Wang JF, Jin Y. A novel theoretical breakup kernel function for bubbles/droplets in a turbulent flow. *Chem Eng Sci*. 2003; 58(20):4629–4637.
42. Luo H, Svendsen HF. Theoretical model for drop and bubble breakup in turbulent dispersions. *AIChE J*. 1996;42(5):1225–1233.
43. Han LC, Luo HA, Liu YJ. A theoretical model for droplet breakup in turbulent dispersions. *Chem Eng Sci*. 2011;66(4):766–776.
44. Andersson R, Andersson B. Modeling the breakup of fluid particles in turbulent flows. *AIChE J*. 2006;52(6):2031–2038.
45. Kuboi R, Komasawa I, Otake T. Behavior of dispersed particles in turbulent liquid flow. *J Chem Eng Jpn*. 1972;5(4):349–355.

46. Lee C-H, Erickson L, Glasgow L. Bubble breakup and coalescence in turbulent gas-liquid dispersions. *Chem Eng Commun.* 1987;59(1–6):65–84.
47. Prince MJ, Blanch HW. Bubble coalescence and break-up in air-sparged bubble-columns. *AIChE J.* 1990;36(10):1485–1499.
48. Hagesaether L, Jakobsen HA, Svendsen HF. A model for turbulent binary breakup of dispersed fluid particles. *Chem Eng Sci.* 2002; 57(16):3251–3267.
49. Solsvik J, Tangen S, Jakobsen HA. On the constitutive equations for fluid particle breakage. *Rev Chem Eng.* 2013;29(5):241–356.
50. Didier B, Francis HH, Norman LJ, Rick R, Jonathan W. Instabilities and Turbulence. *Los Alamos Sci.* 1987;15:145–174.
51. Batchelor GK. *The Theory of Homogeneous Turbulence*. Cambridge: Cambridge University Press, 1953.
52. Pope SB. *Turbulent Flows*. Cambridge: Cambridge University Press, 2000.
53. Perry RH, Green DW. *Perry's Chemical Engineers' Handbook*, *8th ed*. New York: McGraw-Hill, 2008.
54. Tijsseling AS, Vardy AE. Time scales and FSI in unsteady liquid-filled pipe flow. In: Proceedings of the 9th International Conference on Pressure Surges. Chester, United Kingdom, 2004.
55. Hermann S, Klette R. *Multigrid Analysis of Curvature Estimators*. New Zealand: CITR, The University of Auckland, 2003.
56. Coulaloglou CA, Tavlarides LL. Description of interaction processes in agitated liquid-liquid dispersions. *Chem Eng Sci.* 1977;32(11): 1289–1297.
57. Martin M, Montes FJ, Galan MA. Mass transfer rates from oscillating bubbles in bubble columns operating with viscous fluids. *Ind Eng Chem Res.* 2008;47(23):9527–9536.
58. Risso F, Fabre J. Oscillations and breakup of a bubble immersed in a turbulent field. *J Fluid Mech.* 1998;372:323–355.
59. Galinat S, Risso F, Masbernat O, Guiraud P. Dynamics of drop breakup in inhomogeneous turbulence at various volume fractions. *J Fluid Mech.* 2007;578:85–94.
60. Martinez-Bazan C, Montanes JL, Lasheras JC. On the breakup of an air bubble injected into a fully developed turbulent flow. Part 2. Size PDF of the resulting daughter bubbles. *J Fluid Mech.* 1999;401:183–207.
61. Martinez-Bazan C, Montanes JL, Lasheras JC. On the breakup of an air bubble injected into a fully developed turbulent flow. Part 1. Breakup frequency. *J Fluid Mech.* 1999;401:157–182.
62. Maass S, Kraume M. Determination of breakage rates using single drop experiments. *Chem Eng Sci.* 2012;70:146–164.
63. Liao YX, Lucas D. A literature review of theoretical models for drop and bubble breakup in turbulent dispersions. *Chem Eng Sci.* 2009;64(15):3389–3406.
64. Lehr F, Millies M, Mewes D. Bubble-size distributions and flow fields in bubble columns. *AIChE J.* 2002;48(11):2426–2443.
65. Wonham J. Effect of pressure on the viscosity of water. *Nature.* 1967;215(5105):1053–1054.
66. Poling BE, Prausnitz JM, John Paul OC, Reid RC. *The Properties of Gases and Liquids*, Vol. 5. New York: McGraw-Hill, 2001.
67. Massoudi R, King AD. Effect of pressure on the surface tension of water. Adsorption of low molecular weight gases on water at 25.deg. *J Phys Chem.* 1974;78(22):2262–2266.
68. Tennekes H, Lumley JL. *A First Course in Turbulence*. Cambridge: MIT Press, 1972.
69. Wang TF, Wang JF, Jin J. An efficient numerical algorithm for "A novel theoretical breakup kernel function of bubble/droplet in a turbulent flow." *Chem Eng Sci.* 2004;59(12):2593–2595.
70. Sottmann T, Strey R. Ultralow interfacial tensions in water-n-alkane-surfactant systems. *J Chem Phys.* 1997;106(20):8606–8615.
71. Chaumat H, Billet AM, Delmas H. Hydrodynamics and mass transfer in bubble column: influence of liquid phase surface tension. *Chem Eng Sci.* 2007;62(24):7378–7390.
72. Lemoine R, Behkish A, Morsi BI. Hydrodynamic and mass-transfer characteristics in organic liquid mixtures in a large-scale bubble column reactor for the toluene oxidation process. *Ind Eng Chem Res.* 2004;43(19):6195–6212.

Manuscript received Jan. 3, 2014, and revision received Nov. 4, 2014.